Coriandrum sativum seeds as a green low-cost biosorbent for crystal violet dye removal from wastewater

Muhammad Naveed Iqbal[a], Tariq Javed[a,*], Muhammad Babar Taj[b]

[a]*Department of Chemistry, University of Sahiwal, Sahiwal, Pakistan, emails: mtariq@uosahiwal.edu.pk (T. Javed), naveediqbal1605780@gmail.com (M.N. Iqbal)*
[b]*Department of Chemistry, The Islamia University Bahawalpur, 63100, Pakistan, email: dr.taj@iub.edu.pk (M.B. Taj)*

ABSTRACT

Current study focused on *Coriandrum sativum* seeds as a green low-cost biosorbent for crystal violet dye removal from wastewater. Adsorption parameters (such as pH, adsorbent dosage, contact time, adsorbate concentration, and temperature), isotherm models (i.e., Langmuir, Freundlich, and Dubinin–Radushkevich isotherm models), kinetic models (i.e., pseudo-first-order, pseudo-second-order, and intraparticle diffusion models), and thermodynamics study has been studied and investigated. At optimized conditions, that is, pH 7, adsorbent dose of 0.3 g, contact time 50 min, dye concentration of 30 ppm, and 10°C temperature, the maximum dye removal was 75%. Experimental data fitted best to Freundlich isotherm and pseudo-second-order kinetic model. Computed ΔG and ΔH values adjusted adsorption process to be spontaneous and exothermic in nature. Maximum adsorption capacity in current process was found to be 1.8098 mg/g and applicability of established practice with tap water was 72% and regeneration study showed that nearly 71% of adsorbent (*Coriandrum sativum* seeds) was recovered which confirmed the effectiveness of *Coriandrum sativum* seeds for decontamination of crystal violet dye.

Keywords: Crystal violet dye; *Coriandrum sativum* seeds powder; Adsorption; Kinetic models; Isotherm models; Thermodynamics

1. Introduction

Water is one of the most vital and useful requirements in the lives of humans and other living creatures. It is used for variety of purposes and is exposed to various chemicals, thus it might become polluted [1]. Generation of coloured wastewater is an unintended consequence of the invention of various industries, including dyeing, textile, printing, paper, and research labs [2]. Dyes are becoming common water pollutants. The reports of their toxicity are alarming for water resources and the ecosystem [3]. Water pollution is one of the most undesirable environmental problems in the world and this requires solution to purify it [4]. Textile industries produce a lot of wastewaters, which contains several contaminants, including acidic or caustic dissolved solids,

toxic compounds, and many different dyes. Many of these dyes are carcinogenic, mutagenic, teratogenic, and toxic to human beings, fish species, and microorganisms. Hence, their removal from aquatic wastewater is environmentally crucial [5–7].

Effluents released from textile industries are major contributors to water pollution all over the word. Treatment of industrial effluents to remove the toxic colorants is a challenging task to tackle with. These effluents may contain persistent dyes and toxic by-products which are very harmful for health of human being and the quality of aquatic life. Sometimes, due to the higher concentration of dye sunlight cannot penetrate the subsurface of the water in the natural streams, lakes, and rivers which create a negative impact on aquatic life/ phytoplankton and zooplanktons [8]. Crystal

* Corresponding author.

violet (CV) is a water-soluble cationic dye with a complicated structure, also known as basic violet 3, methyl violet 10B and gentian violet, widely used for different dyeing processes for wood, cotton, silk, etc. It has been widely used in various medical fields as an external skin disinfectant in humans, active ingredient in Gram's stain and a bacteriostatic agent [7]. However, it causes severe health problems such as eye irritation, permanent injury to the cornea, breathing difficulty and hypertension [9–11]. During its exposure, it may lead to eyes damage, mental confusion, nausea, vomiting, and methemoglobinemia. Various methods including physicochemical, chemical, and biological methods have been adopted for wastewater treatment. Chemical technology includes such as ferric carbon micro-electrolysis technology, ozonation, photocatalytic oxidation and degradation etc. [12–14]. On the other hand, biochemical technology involves sequencing batch reactors, up-flow anaerobic sludge bed and membrane bioreactor processes. Physicochemical processes such as coagulative precipitation, flotation, membrane separation, electrolysis, and flocculation have been reported as treatment techniques for wastewater from numerous contaminants [15–18]. But these methods require large quantities of reagent and high energy consumption besides generating a huge amount of waste products [19]. Unlike these methods, adsorption-based processes have the possibility of using low-cost and easily available materials which can effectively be exploited for adsorption/removal of pollutants from wastewater. Keeping these aspects in view, many new materials have been studied for the adsorption of dyes from wastewater [20,21].

Activated carbon has become the most widely used adsorbent to remove dyes because it shows good adsorption property and chemical stability. Since operation cost of activated carbon is very high, people are trying to find more economical and efficient adsorbents to treat wastewater and now an alternative has been successfully explored from different agricultural and forestry wastes such as peanut husk [22], banana peel [23], saw dust [24], fish scales [25], coconut coir dust [26], internal almond shell [27], walnut shell [28], MDF waste [29], kudzu [29], bagasse pith, fuller's earth, and silica [30], wheat bran [31], spent tea leaves [32], orange peel [33], meranti saw dust [34], eggshell waste [35], coconut bunch waste [36], mango seed [37], luffa acutangula peel [38] and many fish scale derivatives such as rohu (*Labeo rohita*) [39], coconut husk [40], tilapia (*Oreochromis niloticus*) [41], piau (*Leporinus elongates*) scales [42], potato peel [11], corn stalk [43], olive leaves [44], mango leaves [45], rice husk [46], aloe vera biomass [47], pistachio shells [48], metal-doped TiO_2 [49], acid treated natural oil palm trunk powder (OPTP) [50], acid modified banana peels [51], natural adsorbents, that is, from activated coconut shells, activated cow bones and zeolite [52], dried prickly pear cactus cladodes [53], greensand (glauconite) [54], calcium alginate-multiwall carbon nanotube (CA/MWCNTs) [55], *Chroococcus dispersus* algae [56], greensand [57] and ground nut shell etc. were investigated [58].

Coriander (*Coriandrum sativum*) is a popular spice and a major ingredient of curry powder, an effective antioxidant, and a drug for rheumatism, against worms, and indigestion. Coriander (*Coriandrum sativum*) seeds have also many properties as antimicrobial activity, insecticidal effect, hypolipidemic activity, hypoglycemic action, corrosion inhibition, and adsorption of heavy metals and dyes [59–63].

Aims and objectives of current research were to determine an effective, efficient, and economically feasible method for degradation of toxic crystal violet dye from wastewater by adsorption process using *Coriandrum sativum* and to investigate the effects of various operational parameters on dye removal. Applicability of current practice was checked with tap water. This study also explores the basic mechanism of crystal violet dye removal. At the end, efficiency of *Coriandrum sativum* for crystal violet dye degradation was compared with other available adsorbents.

2. Material and methods

2.1. Preparation of adsorbent

The coriander seeds (*Coriandrum sativum*) were collected from local area, washed with deionized water to remove impurities such as sand and dust, dried in an air at 50°C for 24 h, ground using mortar, and then sieved, until the grain size of particles 200 μm was obtained. The resulted material was stored in clean plastic jars to prevent it from humidity.

2.2. Preparation of dye stock solution

1,000 ppm stock solution of crystal violet dye was prepared by dissolving 1 g of dye in 1,000 mL round bottom flask by adding distilled water up to the mark. Fresh solutions were prepared for study of different parameters by diluting the stock solution.

2.3. Batch adsorption studies

For optimization of different parameters (such as pH, shaking time, adsorbent dose, dye concentration, and temperature) batch adsorption experiment was performed. Each experiment was carried out by keeping one parameter as variable and keeping others as constant. 10 mL of dye solution was used for each experiment. Initial absorbance of solution (before adsorption) was measured by UV-visible spectrophotometer at λ_{max} (i.e., 574 nm) of crystal violet dye and is recorded as C_o. Shaking of mixture was employed for 5 min. When equilibrium was attained then mixture was centrifuged at speed of 3,000 rpm, and dye concentration (after adsorption) was determined spectrophotometrically at the λ_{max} of crystal violet and is recorded as C_e. Percentage removal was calculated by formulae given below:

$$\text{Percentage removal} = \frac{C_o - C_e}{C_o} \times 100 \tag{1}$$

where C_o is the initial dye concentration (mg/L) and C_e is the equilibrium dye concentration (mg/L). Adsorption capacity q_t (mg/g) can be obtained via following formulae:

$$q_t = (C_0 - C_e) \times \frac{V}{m} \tag{2}$$

where '*V*' is the volume of solution and '*m*' is the mass of adsorbent.

3. Results and discussions

3.1. Characterization of adsorbent

Adsorbent was characterized by Fourier-transform infrared spectroscopy (FTIR) and scanning electron microscope (SEM) techniques to determine the different functional groups and surface texture of adsorbent respectively.

3.1.1. Fourier transformed infrared

FTIR analysis of *Coriandrum sativum* seed (CSS) and CSS-CV was carried out using a Perkin Elmer spectrum apparatus version 10.03.07 ATR with the spectral resolution 4.0 cm^{-1}. Both corresponding FTIR spectra were shown in (Fig. 1). A strong peak at 3,415.66 cm^{-1} indicates the presence of hydroxyl group. The presence of aliphatic groups

($-CH_2$ or $-CH_3$) was proved by the peak at 2,925.96 cm^{-1} due to the stretching vibrations of C–H bonds. It can be clearly deduced that the decrease in peak size at 3,416.57 cm^{-1} indicates the involvement of hydroxyl group in the CSS-CV interaction [62].

3.1.2. Scanning electron microscope analysis

Morphology of adsorbent was investigated by using a scanning electron microscope (SEM) (model VEGA3 TESCAN). The obtained SEM micrographs of *Coriandrum sativum* seeds both before and after crystal violet (CV) dye removal process are shown in (Fig. 2), respectively. Before adsorption, *Coriandrum sativum* seed (CSS) had a rough surface having various pores in it (Fig. 2a). However, after adsorption, these cavities were filled with crystal violet (CV) dye molecules as shown in (Fig. 2b). It can be deduced that *Coriandrum sativum* seed (CSS) can act as an excellent adsorbent for crystal violet (CV) dye removal [62].
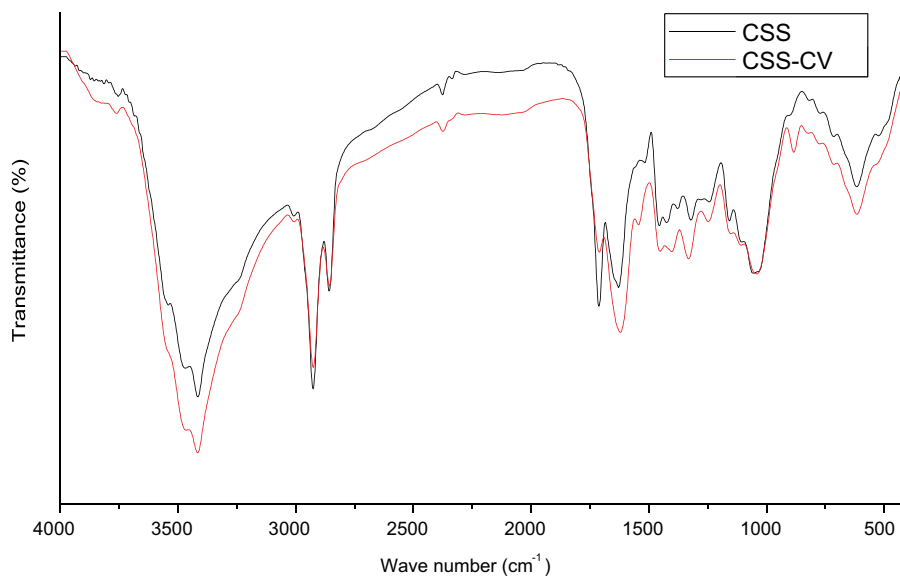

Fig. 1. FTIR spectra of CSS before (------) and after (------) adsorption of crystal violet dye.
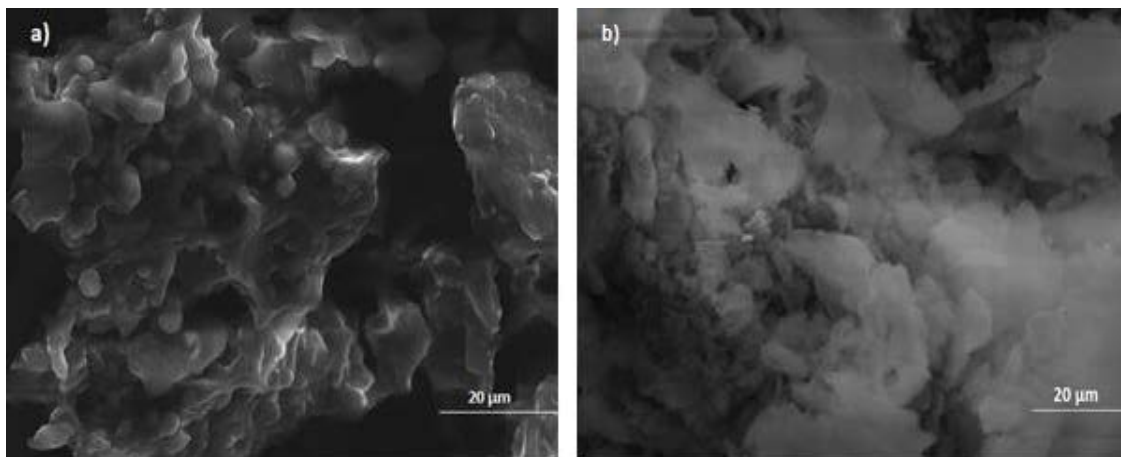

Fig. 2. SEM micrographs of CSS before (a) and after (b) adsorption of crystal violet dye (with resolution of 20 μm).

3.2. Effect of solution pH

Solution pH is amongst the most key factors affecting the sorption capacity of the adsorbent. Effect of solution pH on adsorption of crystal violet (CV) dye on *Coriandrum sativum* (CSS) powder was investigated by varying pH from 1–14. From results it was found that with an increase in pH value up to 7 there was an increase in percentage removal, that is, 75% at neutral pH while at higher pH values (pH > 7), there was a competition between negatively charged hydroxyl ions (in basic solution) and negative surface of *Coriandrum sativum* (CSS) powder (according to the interpretation of the FTIR results) towards crystal violet dye adsorption which decrease percentage removal. While when pH value is below 7 then there were more positive hydrogen ions in the solution which decrease positive dye molecule adsorption on adsorbent surface. Therefore, the optimal value of pH was found to be 7, at which a removal efficiency of 75% was obtained [64]. Effect of solution pH on crystal violet dye removal is shown in Fig. 3.

3.3. Effect of adsorbent dose

To investigate effect of adsorbent amount on crystal violet dye removal, weight of adsorbent changed from 0.1–1.0 g by keeping other parameters constant. From results it became clear that with rise in adsorbent amount, % removal of crystal violet dye upsurges continuously up to 0.3 g (74.765%) after which it becomes constant. This increase in % removal with increase in adsorbent dosage was due to increase in number of available adsorption or exchangeable sites [58,65,66]. The removal percentage increased from 67.957% to 74.765% when weight of adsorbent increased from 0.1 to 0.3 g after which it became constant, that is, 74.765% up to 1.00 g. There is no significant increase in % removal or it became constant after an optimum weight (0.3 g) because all adsorption sites are fully occupied by dye molecules. In other words, we can say that adsorbent dose has direct relation with adsorption of dye molecules. Effects of adsorbent dosage on % removal of dye is given in Fig. 4 [67].

3.4. Effect of contact time

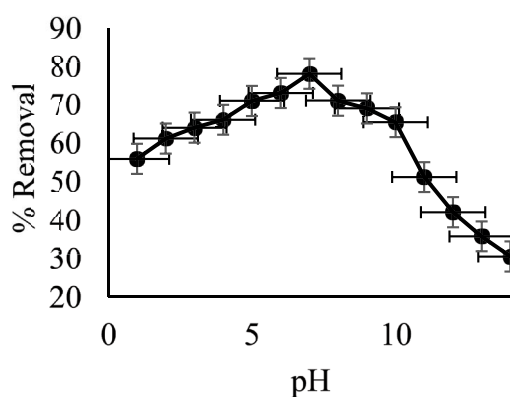Exposure time is the time taken by an adsorbate to be completely adsorbed onto the surface of an adsorbent. To examine the effect of contact time on adsorption process of crystal violet dye, contact time changed from 5–120 min. From experiments, it became clear that maximum time for adsorption of crystal violet dye on surface of *Coriandrum sativum* (CSS) powder was 50 min at which % removal of crystal violet dye was 75%. Thus, optimum time for next experiments was 50 min. Adsorption process was very fast in first 5 min after which there was gradual increase in % removal. Fast reaction in beginning was due to the presence of vacant adsorption spots at the exterior of adsorbent. After some time, all the vacant sites were occupied, and it resulted in small rise in abstraction of dye because at saturation point dye molecules are weakly held on adsorbent surface (probably known as second adsorption layer) [68,69]. In other words at saturation point active sites of adsorbent were impregnated with the dye molecules [70]. The graph showing % removal of dye is given in Fig. 5 [67].

3.5. Effect of dye (adsorbate) concentration

Effect of initial dye concentration on adsorption was studied by changing adsorbate dosage from 5 to 120 ppm. At pH 7, 0.3 g of CSS powder was taken, and varied amount of adsorbate (with exposure time of 50 min) was used to study the % removal of adsorbent towards crystal violet dye. From experiment, it became clear that % removal increased
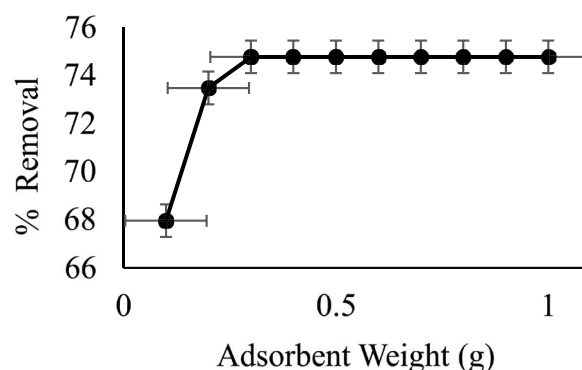
Fig. 4. Plot of adsorbent dose against % removal.
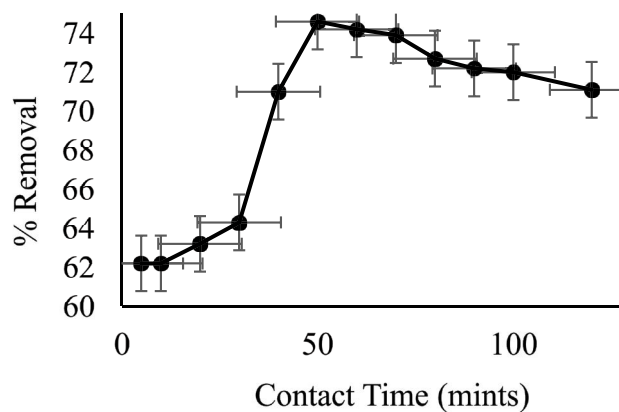
Fig. 3. Plot of pH against % removal.

Fig. 5. Plot of contact time against % removal.

continuously with increase in dye concentration, that is, 76.08% of dye was removed when dye concentration was 30 ppm. After that from 30 to 120 ppm removal percentage decreased constantly from 76.08% to 65.68%. Initial rise in exclusion efficacy was due to the excess amount of adsorbate (crystal violet dye) which adsorbed onto exterior of adsorbent quickly ensuing quick and maximum removal of dye. With increase in dye concentration, there was decrease in percentage removal because at saturation point active sites of adsorbent were impregnated with the dye molecules. Besides repulsion between dye molecules also takes place responsible for decrease in percentage removal of dye [71,72]. As a result, removal efficiency decreases gradually. The graph showing the results is given in Fig. 6 [73]. Experimental results of effect of dye concentration are given in Table 4.

3.6. Effect of temperature

Temperature serves as a key factor affecting the adsorption process of dye and to optimize solution temperature (for maximum adsorption of dye) its value varied from 10°C–60°C while other parameters were constant. Results showed that crystal violet (CV) dye removal using *Coriandrum sativum* (CSS) powder decreased with increase in temperature showing that the process of crystal violet (CV) dye adsorption on *Coriandrum sativum* (CSS) powder is exothermic in nature. Because at elevated temperature dye tends to be soluble in solvent rather than to adsorb on adsorbent surface,
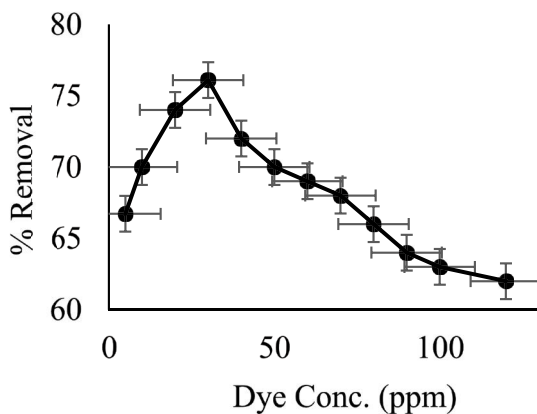
that is, adsorbate-solvent interactions overcome adsorbate–adsorbent interactions leading to decrease in percentage removal of dye. Hence, the process found to be exothermic in nature, similar results were reported by [74–78]. Effect of temperature on crystal violet dye removal is shown in Fig. 7.

3.7. Kinetic study

Various kinetic models were used to optimize adsorption time as well as to investigate mechanism of adsorption of crystal violet dye on *Coriandrum sativum*. These models were pseudo-first-order, pseudo-second-order, and intraparticle diffusion model.

3.7.1. Pseudo-first-order kinetic model

The linear form of pseudo-first-order is given below:

$$\ln\left(q_e - q_t\right) = \ln q_e - K_f t \tag{3}$$

where q_t (mg/g) = amount of adsorbate adsorbed on adsorbent surface at time t, q_e (mg/g) = amount of adsorbate adsorbed on adsorbent surface at equilibrium time, K_f = pseudo-first-order constant. To find values of q_e and K_f a graph was plotted $\ln(q_e - q_t)$ vs. time t (min) [79] shown in Fig. 8. R^2 is a correlation coefficient that is commonly used to verify a better kinetics model. In general, kinetic model with a higher R^2 value is more widely accepted [80].

From results, it was found that R^2 value for pseudo-first-order kinetic model was 0.990 (less than 1). Additionally, there was greater difference amongst calculated, that is, 0.005 mg/g and experimental, that is, 0.171 mg/g q_e values showing that current adsorption process does not follow pseudo-first-order kinetic model.

3.7.2. Pseudo-second-order kinetic model

Linear form of pseudo-second-order model is given below:

$$\frac{t}{q_t} = \frac{1}{K_s q_e^2} + \frac{t}{q_e} \tag{4}$$

Fig. 6. Plot of dye concentration against % removal.
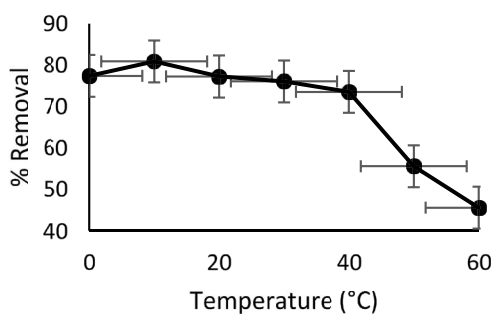
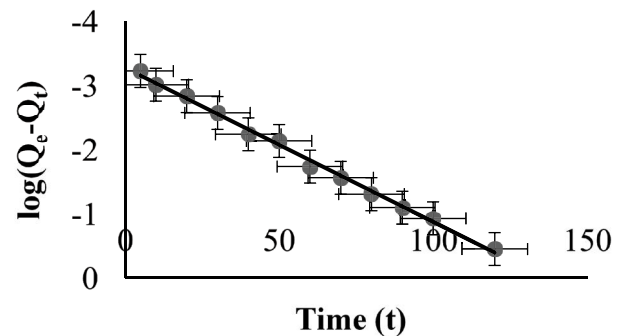Fig. 7. Plot of temperature against % removal.

Fig. 8. Plot of pseudo-first-order model for adsorption of crystal violet by *Coriandrum sativum*.

where q_t (mg/g) = amount of adsorbate adsorbed on adsorbent surface at time t, q_e (mg/g) = amount of adsorbate adsorbed on adsorbent surface at equilibrium time, K_s (g/mg min) = pseudo-second-order rate constant. The values of q_e and K_s were found by plotting a graph of t/q_t (min/g mg) vs. time (min) [81] shown in Fig. 9.

From results it became clear that value of coefficient of determination of pseudo-second-order model is greater than that of pseudo-first-order kinetic model, that is, 0.998 and there is a smaller difference between calculated (0.160) and experimental (0.171) q_e value indicating that data fits best to pseudo-second-order kinetic model.

3.7.3. Intraparticle diffusion model

Weber and Morris proposed this model for determining the diffusion mechanism and rate controlling step in kinetics of adsorption. Mathematical form of this model can be represented as:

$$q_t = K_{id}t^{0.5} + I \tag{5}$$

where q_t (mg/g) = quantity of adsorbate adsorbed at time 't', I = thickness of layer and K_{id} (mg/g min$^{1/2}$) = intraparticle diffusion constant [9]. A plot of intraparticle diffusion model is shown in Fig. 10. Plot obtained by data is not linear. It means that only intra particle diffusion model is not the rate limiting step, but other kinetic models are also involved in control of adsorption speed.

Similar trend was observed with various adsorbents [9,82,83]. Pseudo-second-order model has benefit that adsorption at equilibrium and initial adsorption rate can be calculated from itself, with no need of getting equilibrium sorption capacity from trials [84]. Comparison of kinetic models is given in Table 1.

3.8. Adsorption isotherm

To determine the best suited isotherm model in the adsorption process, concentration data from the experiment is analyzed using various isotherm models. Langmuir, Freundlich, and Dubinin–Radushkevich (D-R) isotherm models were studied in current research.
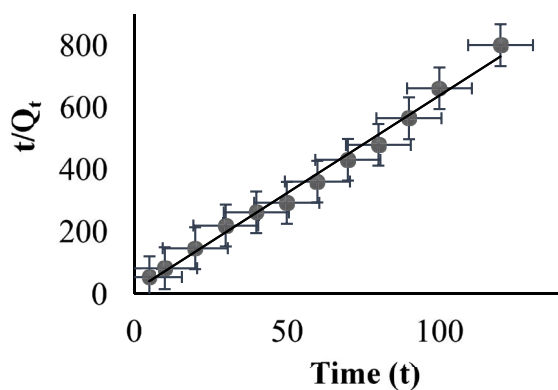
Fig. 9. A plot of pseudo-second-order model for adsorption of crystal violet by CSS.

3.8.1. Langmuir adsorption isotherm model

This isotherm deals with interaction of adsorbate on adsorbent surface without interacting with each other. It deals with monolayer adsorption. Linear form of Langmuir model is given as below:

$$\frac{1}{q_e} = \frac{1}{q_{max}} + \left(\frac{1}{q_{max}K_L}\right)\frac{1}{C_e} \quad [85] \tag{6}$$

where K_L = Langmuir constant (dm^3/mol) and q_{max} = monolayer adsorption capacity (mg/g). This equation can be simply written as:

$$\frac{C_e}{q_e} = \frac{1}{q_{max}K_L} + \left(\frac{C_e}{q_{max}}\right) \quad [86] \tag{7}$$

In general, q_{max} and K_L are functions of pH, ionic medium, and adsorbate ionic strength. When we plot a graph between C_e (mg/L)/q_e (mg/g) and C_e (mg/L), a straight line will be obtained [81]. The Langmuir isotherm results for adsorption of crystal violet dye on to the surface of *Coriandrum sativum* from aqueous solution are shown in Fig. 11. R^2 value was 0.994 which is very similar to unity, indicating that the current adsorption process is promising.

3.8.2. Freundlich adsorption isotherm model

Freundlich model provides relationship between adsorption of adsorbate on adsorbent surface with pressure of gas by equation given below:
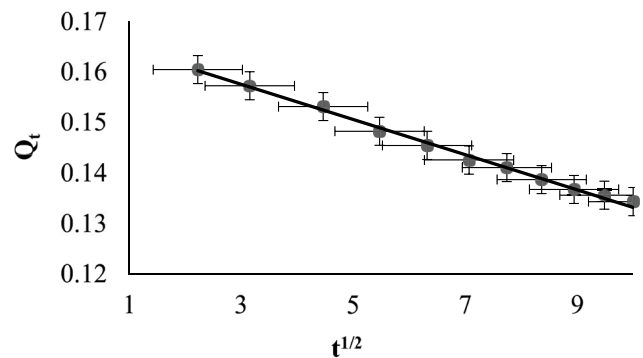
Fig. 10. A plot of intraparticle diffusion model for adsorption of crystal violet dye.

Table 1
Comparison of kinetic parameters of three models (pseudo-first-order, pseudo-second-order, and intraparticle diffusion model)

Pseudo-first-order	Pseudo-second-order	Intraparticle diffusion model
q_e (mg/g) = 0.005	q_e (mg/g) = 0.160	q_e (mg/g) = 0.191
R^2 = 0.990	R^2 = 0.998	R^2 = 0.996
K_1 (min^{-1}) = 0.055	K_1 (min^{-1}) = 0.591	K_{id} = 0.003

$$q_e = K_F P \tag{8}$$

Linear form of Freundlich adsorption isotherm model is:

$$\ln q_e = K_F + \frac{1}{n} \ln P \tag{9}$$

In case of solution, this equation can be written as:

$$\ln q_e = K_F + \frac{1}{n} \ln C_e \tag{10}$$

where K_F = Freundlich constant, n = slope, q_e (mg/g) = amount of adsorbate adsorbed per gram of an adsorbent. Straight line graph is obtained when we plot $\ln q_e$ vs. $\ln C_e$. From intercept and slope of graph K_F and "n" can be determined [81]. The Freundlich isotherm graph is shown in Fig. 12. R^2 value for Freundlich isotherm model is 0.999 (higher than that of Langmuir isotherm value) which is very close to 1 which confirmed that statistical data follows Freundlich isotherm model.

3.8.3. Dubinin–Radushkevich isotherm model

This isotherm is an empirical model that explains mechanism of adsorption with a Gaussian surface distribution on a heterogeneous surface [87]. The Dubinin–Radushkevich isotherm is temperature dependent. The equation for Dubinin–Radushkevich is:
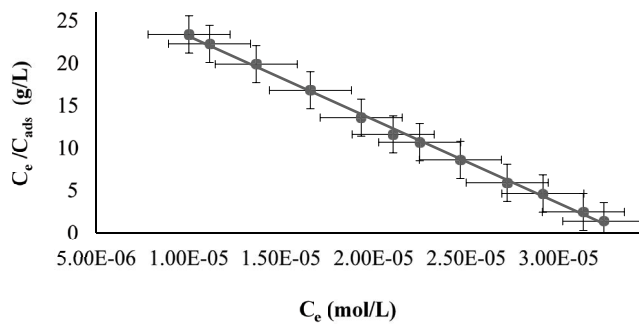

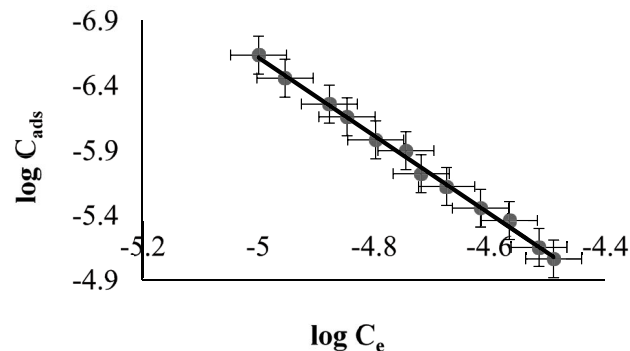Fig. 11. A plot of Langmuir isotherm model.

Fig. 12. A plot of Freundlich isotherm model.

$$\ln q_e = \ln q_{DR} - \beta \varepsilon^2 \tag{11}$$

where β = activity coefficient, $\ln q_{DR}$ = imaginary inundation capacity, ε is Polanyi potential given as follows:

$$\varepsilon = RT \ln \left(1 + \frac{1}{C_e} \right) \tag{12}$$

where T = temperature, R is general gas constant. Energy of transference of one mole of solute from infinity to adsorbent exterior is mean sorption energy denoted by β.

$$\beta = \frac{1}{\sqrt{2\beta}} \tag{13}$$

where β = activity coefficient [81]. D-R plot is shown in Fig. 13. Value of R^2 for D-R isotherm model is 0.986 which is less than that of Freundlich adsorption isotherm model and value of energy 1.51 (kJ/mol) indicated that current process is chemical as well physical in nature.

When we compare results of different isotherm models (Table 2) we found that experimental data fits best to Freundlich isotherm model rather than Langmuir and D-R isotherm models due to its greater R^2 value. Obtained adsorption isotherm showed that current process of adsorption of crystal violet dye on coconut husk powder is
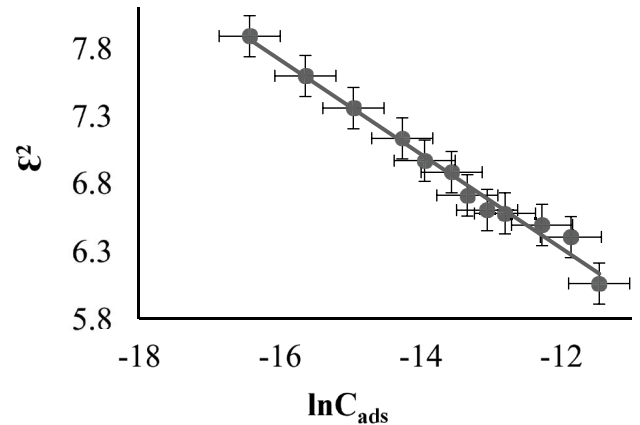
Fig. 13. Graph of D-R isotherm model.

Table 2
Comparison of isotherm models (Langmuir, Freundlich and Dubinin–Radushkevich model)

Isotherm model	Parameters		R^2
Freundlich	n (L/g)	K_f (mg/g)	0.999
	0.2171	1.8098	
Langmuir	Q_o (mg/g)	b (dm³/mol)	0.994
	1.01995×10^{-8}	8.5749×10^{-7}	
Dubinin–Radushkevich	β = (kJ²/mol²)	ε^2 (kJ/mol)	0.986
	0.348	1.51099	

favorable [70] with physical adsorption dominating over chemical adsorption [84]. Comparison of adsorption capacities of various adsorbents is given in Table 3 which showed that *Coriandrum sativum* is an excellent adsorbent for adsorption of crystal violet dye as its q_e value is higher as compared to other adsorbents.

3.9. Thermodynamic study

The temperature impact on the adsorption process is another important component that determines whether the adsorption system is exothermic or endothermic and alters the adsorbent's adsorption capability [9]. Free energy (ΔG), free enthalpy (ΔH) and entropy (ΔS) were estimated by the equations given below.

$$\Delta G = -RT \ln K_c \tag{14}$$

$$K_c = \frac{q_e}{C_e} \tag{15}$$

Table 3
Comparison of adsorption capacities of various adsorbents for crystal violet dye adsorption

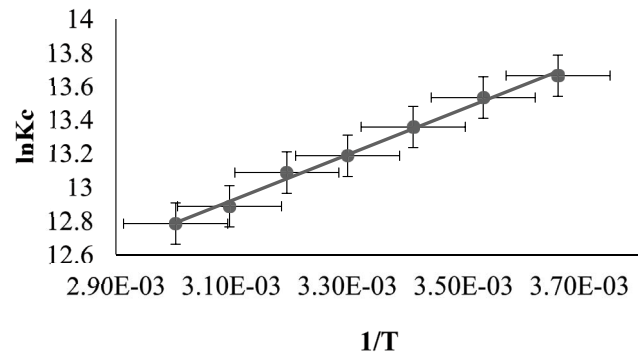| Adsorbent	Adsorption capacity (mg/g)	Reference
Coriander seeds	1.8098	Present work
Keratin nanoparticles	1.57	[88]
Ground nutshell	0.524	[89]
Activated carbon	18.47	[10]
Date palm fiber	1.31	[75]
Coniferous *Pinus* bark	0.72	[90]
Nanomagnetic iron oxide	16.51	[91]
Cedrus deodara sawdust	0.673	[9]

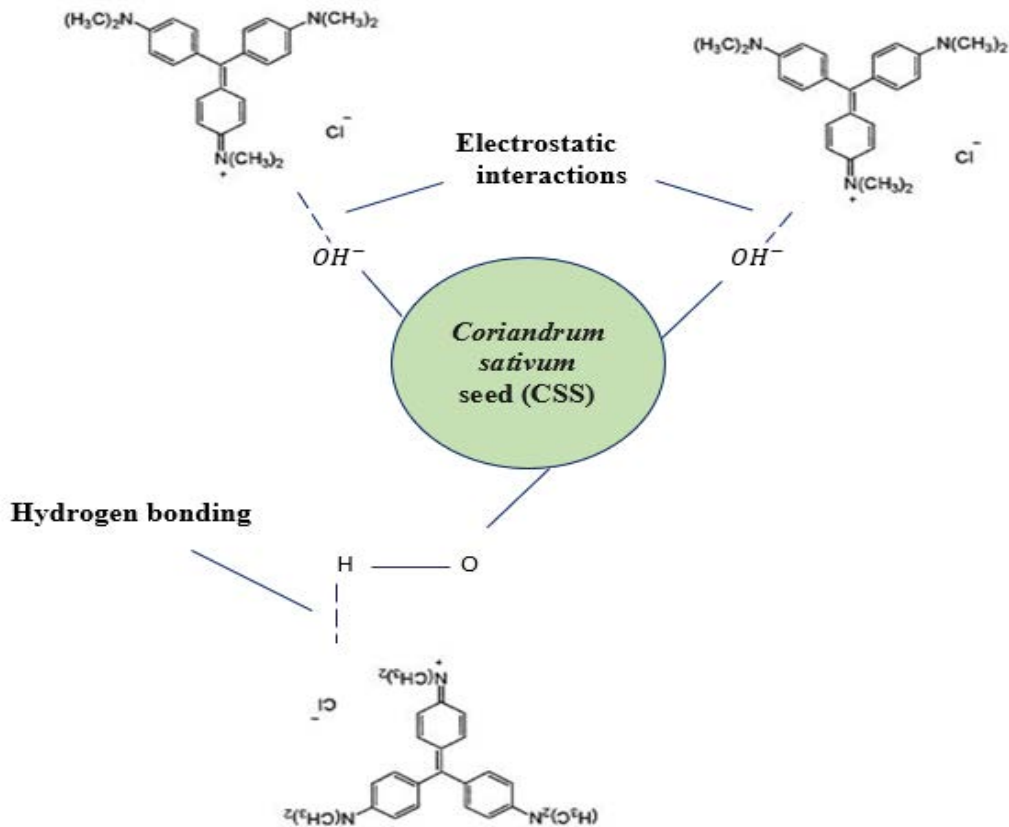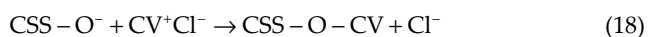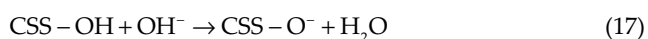Fig. 14. Van't Hoff plot of crystal violet dye adsorption by *Coriandrum sativum*.

Fig. 15. Mechanism of crystal violet dye adsorption on *Coriandrum sativum*.

$$\Delta G = \Delta H - T\Delta S \quad [92] \tag{16}$$

When a graph is plotted between $\ln K_c$ and $1/T$ then we will get a straight-line from which ΔH and ΔS can be determined from its s slope and intercept respectively. R, universal gas constant = 8.31 J/mol K and T = temperature in Kelvin [92]. Van't Hoff plot is given in Fig. 14. Because of the negative value of ΔG, adsorption seems to be spontaneous in nature and randomness of process increased as confirmed by positive ΔS [93–95].

3.10. Mechanism of adsorption

From FTIR results it became clear that adsorption of crystal violet dye on *Coriandrum sativum* seeds (CSS) (adsorbent) was basically due to interactions between ionizable functional groups of adsorbents such as hydroxyl group etc. and crystal violet dye molecules. Strong electrostatic interactions between dye molecules (CV^+Cl^-) and specific functional groups of adsorbents are responsible for breaking dye intra-molecular bonds and hence their removal from wastewater. Mechanism of adsorption by hydroxyl functional group is as follows:

$$CSS-OH + OH^- \rightarrow CSS-O^- + H_2O \tag{17}$$

$$CSS-O^- + CV^+Cl^- \rightarrow CSS-O-CV + Cl^- \tag{18}$$

where, CSS represents *Coriandrum sativum* seeds (adsorbent) and CV^+Cl^- represents crystal violet dye molecules. Mechanism of crystal violet dye adsorption on *Coriandrum sativum* is shown in Fig. 15.

3.11. Desorption study

When 1 M HNO_3 was added to the loaded dye solution, pH of the solution dropped. As a result, bond weakens between dye and adsorbent leading to desorption of dye from surface of adsorbent. Nevertheless, removal efficacy of adsorbent decreased after regeneration but can be reused for treatment [9,70,92,96–98].

3.12. Applicability of developed procedure with tap water

Current adsorption process was also studied with tap water to study the effect of various cations and anions [9]

(e.g., phosphates, sulphates, nitrates, calcium, potassium ions etc.) on crystal violet dye adsorption on *Coriandrum sativum* under optimized conditions and results showed that nearly 75% of dye was removed in this way which showed that *Coriandrum sativum* seed (CSS) is a potential adsorbent for removal of crystal violet dye from wastewater.

4. Conclusion

- This research paper aimed to investigate the potential of *Coriandrum sativum* as an adsorbent for crystal violet dye removal from wastewater and to optimize different adsorption parameters for maximum adsorption of dye.
- Results showed maximum percentage degradation, that is, 81% at optimized conditions such as pH 7 solution, 0.3 g adsorbent dose, with 50 min of exposure time and 30 ppm of dye concentration at 10°C solution temperature.
- Results of characterization confirmed that hydroxyl group and heterogenous adsorbent surface was responsible for crystal violet dye adsorption on *Coriandrum sativum*.
- Results of concentration and kinetic data confirmed that experimental data fitted well to Freundlich isotherm model (R^2 = 0.999) and pseudo-second-order kinetic model (R^2 = 0.998).
- Computed ΔG and ΔH values confirmed adsorption process to be spontaneous and exothermic in nature.
- Applicability of established procedure with tap water or real system was 75% which showed the effectiveness of *Coriandrum sativum* for removal of crystal violet dye from wastewater.

Conflicts of interest

Authors state no competing financial concerns to influence the work described in this research.

Availability of data and material (data transparency)

Authors will ensure data transparency.

Authors' contributions

All authors contribute equally to the manuscript.

Data availability

Data that support this study are available in the article and accompanying supplementary file.

Symbols

q_t	—	Adsorption capacity at time 't', mg/g
q_e	—	Adsorption capacity at equilibrium, mg/g
C_o	—	Initial concentration of dye, mg/L
C_e	—	Equilibrium concentration of dye, mg/L
V	—	Volume of dye solution taken, mL
m	—	Mass of adsorbent, g
K_F	—	Pseudo-first-order rate constant, mg/g
K_s	—	Pseudo-second-order rate constant, mg/g
K_L	—	Langmuir constant, dm^3/mol

Table 4
Calculated thermodynamic parameters

Temperature (K)	ΔG (kJ/mol)	ΔH (kJ/mol)	ΔS (J/mol K)
273	–29.674	11.750	0.152
283	–31.152	11.750	0.152
293	–31.836	11.750	0.149
303	–32.796	11.750	0.147
313	–33.625	11.750	0.145
323	–33.331	11.750	0.140
333	–33.815	11.750	0.137

b	—	Langmuir equilibrium constant, L/mol
R_L	—	Dimensionless constant, separation factor parameter
n	—	Intensity of adsorption, L/g
β	—	Constant related to adsorption energy or activity coefficient, kJ²/mol²
q_{DR}	—	Imaginary inundation capacity
ε^2	—	Polanyi potential, kJ/mol
C_{id}	—	Intraparticle rate constant, mg/g min$^{1/2}$
C_{ads}	—	Adsorbed concentration, mg/L
C_{eq}	—	Unabsorbed quantity of adsorbate in solution at equipoise, mg/L
T	—	Temperature, K
R	—	Universal gas constant = 8.31 J/mol K
ΔG	—	Change in Gibbs free energy, kJ/mol
ΔH	—	Change in enthalpy, kJ/mol
ΔS	—	Change in entropy, J/mol K

References

[1] R. Foroutan, S.J. Peighambardoust, S.H. Peighambardoust, M. Pateiro, J.M. Lorenzo, Adsorption of crystal violet dye using activated carbon of lemon wood and activated carbon/Fe₃O₄ magnetic nanocomposite from aqueous solutions: a kinetic, equilibrium and thermodynamic study, Molecules, 26 (2021) 2241, doi: 10.3390/molecules26082241.

[2] R. Fabryanty, C. Valencia, F.E. Soetaredjo, J.N. Putro, S.P. Santoso, A. Kurniawan, Y.-H. Ju, S. Ismadji, Removal of crystal violet dye by adsorption using bentonite – alginate composite, J. Environ. Chem. Eng., 5 (2017) 5677–5687.

[3] U. Baig, M.K. Uddin, M. Gondal, Removal of hazardous azo dye from water using synthetic nano adsorbent: facile synthesis, characterization, adsorption, regeneration and design of experiments, Colloids Surf., A, 584 (2020) 124031, doi: 10.1016/j.colsurfa.2019.124031.

[4] L.B.L. Lim, N. Priyantha, T. Zehra, C.W. Then, C.M. Chan, Adsorption of crystal violet dye from aqueous solution onto chemically treated *Artocarpus odoratissimus* skin: equilibrium, thermodynamics, and kinetics studies, Desal. Water Treat., 57 (2016) 10246–10260.

[5] T. Maneerung, J. Liew, Y. Dai, S. Kawi, C. Chong, C.-H. Wang, Activated carbon derived from carbon residue from biomass gasification and its application for dye adsorption: kinetics, isotherms and thermodynamic studies, Bioresour. Technol., 200 (2016) 350–359.

[6] F. Sakr, S. Alahiane, A. Sennaoui, M. Dinne, I. Bakas, A. Assabbane, Removal of cationic dye (Methylene Blue) from aqueous solution by adsorption on two type of biomaterial of South Morocco, Mater. Today: Proc., 22 (2020) 93–96.

[7] A. Asfaram, M. Ghaedi, S. Hajati, A. Goudarzi, E.A. Dil, Screening and optimization of highly effective ultrasound-assisted simultaneous adsorption of cationic dyes onto Mn-doped Fe₃O₄-nanoparticle-loaded activated carbon, Ultrason. Sonochem., 34 (2017) 1–12.

[8] S. Pashaei-Fakhri, S.J. Peighambardoust, R. Foroutan, N. Arsalani, B. Ramavandi, Crystal violet dye sorption over acrylamide/graphene oxide bonded sodium alginate nanocomposite hydrogel, Chemosphere, 270 (2021) 129419, doi: 10.1016/j.chemosphere.2020.129419.

[9] M. Batool, T. Javed, M. Wasim, S. Zafar, M.I. Din, Exploring the usability of *Cedrus deodara* sawdust for decontamination of wastewater containing crystal violet dye, Desal. Water Treat., 224 (2021) 433–448.

[10] T. Aysu, M.M. Küçük, Removal of crystal violet and methylene blue from aqueous solutions by activated carbon prepared from *Ferula orientalis*, Int. J. Environ. Sci. Technol., 12 (2015) 2273–2284.

[11] S. Lairini, K. El Mahtal, Y. Miyah, K. Tanji, S. Guissi, S. Boumchita, F. Zerrouq, The adsorption of Crystal violet from aqueous solution by using potato peels (*Solanum tuberosum*): equilibrium and kinetic studies, J. Mater. Environ. Sci., 8 (2017) 3252–3261.

[12] S.A. Sallam, G.M. El-Subruiti, A.S. Eltaweil, Facile synthesis of Ag–γ-Fe₂O₃ superior nanocomposite for catalytic reduction of nitroaromatic compounds and catalytic degradation of methyl orange, Catal. Lett., 148 (2018) 3701–3714.

[13] X. Xu, Y. Cheng, T. Zhang, F. Ji, X. Xu, Treatment of pharmaceutical wastewater using interior micro-electrolysis/ Fenton oxidation-coagulation and biological degradation, Chemosphere, 152 (2016) 23–30.

[14] G.M. El-Subruiti, A.S. Eltaweil, S.A. Sallam, Synthesis of active MFe₂O₄/γ-Fe₂O₃ nanocomposites (metal = Ni or Co) for reduction of nitro-containing pollutants and methyl orange degradation, Nano, 14 (2019) 1950125, doi: 10.1142/S179329201950125X.

[15] M. Rashad, H.A. Al-Aoh, Promising adsorption studies of bromophenol blue using copper oxide nanoparticles, Desal. Water Treat., 139 (2019) 360–368.

[16] S. Mukherjee, L. Weihermüller, W. Tappe, D. Hofmann, S. Köppchen, V. Laabs, H. Vereecken, P. Burauel, Sorption– desorption behaviour of bentazone, boscalid and pyrimethanil in biochar and digestate based soil mixtures for biopurification systems, Sci. Total Environ., 559 (2016) 63–73.

[17] Z. Thong, J. Gao, J.X.Z. Lim, K.-Y. Wang, T.-S. Chung, Fabrication of loose outer-selective nanofiltration (NF) polyethersulfone (PES) hollow fibers via single-step spinning process for dye removal, Sep. Purif. Technol., 192 (2018) 483–490.

[18] Y. Yuan, H. Zhang, G. Pan, Flocculation of cyanobacterial cells using coal fly ash modified chitosan, Water Res., 97 (2016) 11–18.

[19] F.E. Titchou, R.A. Akbour, A. Assabbane, M. Hamdani, Removal of cationic dye from aqueous solution using Moroccan pozzolana as adsorbent: isotherms, kinetic studies, and application on real textile wastewater treatment, Groundwater Sustainable Dev., 11 (2020) 100405, doi: 10.1016/j.gsd.2020.100405.

[20] M. Benafqir, A. Hsini, M. Laabd, T. Laktif, A.A. Addi, A. Albourine, N. El Alem, Application of density functional theory computation (DFT) and process capability study for performance evaluation of orthophosphate removal process using polyaniline@hematite-titaniferous sand composite (PANI@HTS) as a substrate, Sep. Purif. Technol., 236 (2020) 116286, doi: 10.1016/j.seppur.2019.116286.

[21] X.X. Liang, A.M. Omer, Z.-H. Hu, Y.-G. Wang, D. Yu, X.-K. Ouyang, Efficient adsorption of diclofenac sodium from aqueous solutions using magnetic amine-functionalized chitosan, Chemosphere, 217 (2019) 270–278.

[22] Y. Song, Y. Liu, S. Chen, H. Xu, Y. Liao, Sunset yellow adsorption by peanut husk in batch mode, Fresenius Environ. Bull., 23 (2014) 1074–1079.

[23] F. Temesgen, N. Gabbiye, O. Sahu, Biosorption of reactive red dye (RRD) on activated surface of banana and orange peels: economical alternative for textile effluent, Surf. Interfaces, 12 (2018) 151–159.

[24] S. Banerjee, M. Chattopadhyaya, Adsorption characteristics for the removal of a toxic dye, tartrazine from aqueous solutions by a low cost agricultural by-product, Arabian J. Chem., 10 (2017) S1629–S1638.

[25] A. Bukhari, T. Javed, M.N. Haider, Adsorptive exclusion of crystal violet dye from wastewater by using fish scales as an adsorbent, J. Dispersion Sci. Technol., (2022) 1–12, doi: 10.1080/01932691.2022.2059506.

[26] U. Etim, S. Umoren, U. Eduok, Coconut coir dust as a low cost adsorbent for the removal of cationic dye from aqueous solution, J. Saudi Chem. Soc., 20 (2016) S67–S76.

[27] D. Sana, S. Jalila, A comparative study of adsorption and regeneration with different agricultural wastes as adsorbents for the removal of methylene blue from aqueous solution, Chin. J. Chem. Eng., 25 (9) (2017) 1282–1287.

[28] Y. Miyah, A. Lahrichi, M. Idrissi, A. Khalil, F. Zerrouq, Adsorption of methylene blue dye from aqueous solutions onto walnut shells powder: equilibrium and kinetic studies, Surf. Interfaces, 11 (2018) 74–81.

[29] R.P. Matthews, Adsorption of Dies Using Kudzu, Peanut Hulls and MDF Sawdust, Thesis (Ph.D.), Queen's University

of Belfast, 2003. Available at: https://ethos.bl.uk/OrderDetails. do?uin=uk.bl.ethos.397874

[30] S. Allen, Types of Adsorbent Materials, CRC Press, Boca Raton, FL, 1996.

[31] M.T. Sulak, E. Demirbas, M. Kobya, Removal of Astrazon Yellow 7GL from aqueous solutions by adsorption onto wheat bran, Bioresour. Technol., 98 (2007) 2590–2598.

[32] N. Nasuha, B. Hameed, A.T.M. Din, Rejected tea as a potential low-cost adsorbent for the removal of methylene blue, J. Hazard. Mater., 175 (2010) 126–132.

[33] M. Arami, N.Y. Limaee, N.M. Mahmoodi, N.S. Tabrizi, Removal of dyes from colored textile wastewater by orange peel adsorbent: equilibrium and kinetic studies, J. Colloid Interface Sci., 288 (2005) 371–376/

[34] A. Ahmad, M. Rafatullah, O. Sulaiman, M.H. Ibrahim, R. Hashim, Scavenging behaviour of meranti sawdust in the removal of methylene blue from aqueous solution, J. Hazard. Mater., 170 (2009) 357–365.

[35] H. Daraei, A. Mittal, M. Noorisepehr, F. Daraei, Kinetic and equilibrium studies of adsorptive removal of phenol onto eggshell waste, Environ. Sci. Pollut. Res., 20 (2013) 4603–4611.

[36] B. Hameed, D. Mahmoud, A. Ahmad, Equilibrium modeling and kinetic studies on the adsorption of basic dye by a low-cost adsorbent: coconut (*Cocos nucifera*) bunch waste, J. Hazard. Mater., 158 (2008) 65–72.

[37] W.S. Alencar, E. Acayanka, E.C. Lima, B. Royer, F.E. de Souza, J. Lameira, C.N. Alves, Application of *Mangifera indica* (mango) seeds as a biosorbent for removal of Victazol Orange 3R dye from aqueous solution and study of the biosorption mechanism, Chem. Eng. J., 209 (2012) 577–588.

[38] H.W. Ng, L.Y. Lee, W.L. Chan, S. Gan, N. Chemmangattuvalappil, *Luffa acutangula* peel as an effective natural biosorbent for malachite green removal in aqueous media: equilibrium, kinetic and thermodynamic investigations, Desal. Water Treat., 57 (2016) 7302–7311.

[39] S. Chowdhury, P. Das Saha, U. Ghosh, Fish (*Labeo rohita*) scales as potential low-cost biosorbent for removal of malachite green from aqueous solutions, Biorem. J., 16 (2012) 235–242.

[40] M.S. Imran, T. Javed, I. Areej, M.N. Haider, Sequestration of crystal violet dye from wastewater using low-cost coconut husk as a potential adsorbent, Water Sci. Technol., 85 (2022) 2295–2317.

[41] C. Ribeiro, F.B. Scheufele, F.R. Espinoza-Quinones, A.N. Módenes, M.G.C. da Silva, M.G.A. Vieira, C.E. Borba, Characterization of *Oreochromis niloticus* fish scales and assessment of their potential on the adsorption of reactive blue 5G dye, Colloids Surf., A, 482 (2015) 693–701.

[42] E.F.S. Vieira, A.R. Cestari, W.A. Carvalho, C. dos S. Oliveira, R.A. Chagas, The use of freshwater fish scale of the species *Leporinus elongatus* as adsorbent for anionic dyes: an isothermal calorimetric study, J. Therm. Anal. Calorim., 109 (2012) 1407–1412.

[43] U.L. Muhammad, Z.U. Zango, H.A. Kadir, Crystal violet removal from aqueous solution using corn stalk biosorbent, Sci. World J., 14 (2019) 133–138.

[44] K.M. Elsherif, A. El-Dali, A.A. Alkarewi, A.M. Ewlad-Ahmed, A. Treban, Adsorption of crystal violet dye onto olive leaves powder: equilibrium and kinetic studies, Chem. Int., 7 (2021) 79–89.

[45] G. Vyavahare, P. Jadhav, J. Jadhav, R. Patil, C. Aware, D. Patil, A. Gophane, Y.-H. Yang, R. Gurav, Strategies for crystal violet dye sorption on biochar derived from mango leaves and evaluation of residual dye toxicity, J. Cleaner Prod., 207 (2019) 296–305.

[46] N.T. Luyen, H.X. Linh, T.Q. Huy, Preparation of rice husk biochar-based magnetic nanocomposite for effective removal of crystal violet, J. Electron. Mater., 49 (2020) 1142–1149.

[47] A. Ahmad, D. Lokhat, M. Rafatullah, A. Khatoon, S. Setapar, *Aloe vera* biomass containing cellulosic moieties used as sustainable adsorbents for the removal of crystal violet dye from aqueous solution, Desal. Water Treat., 170 (2019) 337–348.

[48] A. Rafiee, S. Ghanavati Nasab, A. Teimouri, Synthesis and characterization of pistachio shell/nanodiopside nanocomposite

[49] and its application for removal of Crystal Violet dye from aqueous solutions using central composite design, Int. J. Environ. Anal. Chem., 100 (2020) 1624–1649.

[49] U. Khalid, P. Tabassum, M.A. Khan, M.N.M. Ibrahim, A. Akil, R. Mohd, Degradation of organic pollutants using metal-doped TiO_2 photocatalysts under visible light: a comparative study, Desal. Water Treat., 161 (2019) 275–282.

[50] A. Ahmad, M. Rafatullah, M. Vakili, S.H. Mohd-Setapar, Equilibrium and kinetic studies of methyl orange adsorption onto chemically treated oil palm trunk powder, Environ. Eng. Manage. J., 17 (2018), doi: 10.30638/eemj.2018.294.

[51] A.A. Oyekanmi, A. Ahmad, K. Hossain, M. Rafatullah, Adsorption of Rhodamine b dye from aqueous solution onto acid treated banana peel: response surface methodology, kinetics and isotherm studies, PLoS One, 14 (2019) e0216878, doi: 10.1371/journal.pone.0216878.

[52] A.A. Oyekanmi, A.A.A. Latiff, Z. Daud, R.M.S.R. Mohamed, N. Aziz, N. Ismail, M. Rafatullah, A. Ahmad, K. Hossain, Adsorption of pollutants from palm oil mill effluent using natural adsorbents: optimization and isotherm studies, Desal. Water Treat., 169 (2019) 181–190.

[53] A. Ahmad, S.H. Mohd-Setapar, C.S. Chuong, A. Khatoon, W.A. Wani, R. Kumar, M. Rafatullah, Recent advances in new generation dye removal technologies: novel search for approaches to reprocess wastewater, RSC Adv., 5 (2015) 30801–30818.

[54] D. Naghipour, K. Taghavi, M. Ashournia, J. Jaafari, R. Arjmand Movarrekh, A study of Cr(VI) and NH_{4+} adsorption using greensand (glauconite) as a low-cost adsorbent from aqueous solutions, Water Environ. Res., 34 (2020) 45–56.

[55] S.D. Ashrafi, G.H. Safari, K. Sharafi, H. Kamani, J. Jaafari, Adsorption of 4-Nitrophenol on calcium alginate-multiwall carbon nanotube beads: modeling, kinetics, equilibriums and reusability studies, Int. J. Biol. Macromol., 185 (2021) 66–76.

[56] J. Jaafari, K. Yaghmaeian, Response surface methodological approach for optimizing heavy metal biosorption by the blue-green alga *Chroococcus disperses*, Desal. Water Treat., 142 (2019) 225–234.

[57] D. Naghipour, R.A. Movarrekh, K. Taghavi, J. Jaafari, Adsorption of Fe(II) and Mn(II) using glauconitic greensands from aqueous solution, Desal. Water Treat., 190 (2020) 237–246.

[58] Z.U. Zango, S.S. Imam, Evaluation of microcrystalline cellulose from groundnut shell for the removal of crystal violet and methylene blue, Nanosci. Nanotechnol., 8 (2018) 1–6.

[59] L. Kadiri, M. Galai, M. Ouakki, Y. Essaadaoui, A. Ouass, M. Cherkaoui, E.-H. Rifi, A. Lebkiri, *Coriandrum sativum* L seeds extract as a novel green corrosion inhibitor for mild steel in 1.0 M hydrochloric and 0.5 M sulfuric solutions, Anal. Bioanal. Chem. Res., 10 (2018) 249–268.

[60] S. Mandal, M. Mandal, Coriander (*Coriandrum sativum* L.) essential oil: chemistry and biological activity, Asian Pac. J. Trop. Biomed., 5 (2015) 421–428.

[61] H. Fatemi, B. Esmaiel Pour, M. Rizwan, Foliar application of silicon nanoparticles affected the growth, vitamin C, flavonoid, and antioxidant enzyme activities of coriander (*Coriandrum sativum* L.) plants grown in lead (Pb)-spiked soil, Environ. Sci. Pollut. Res., 28 (2021) 1417–1425.

[62] L. Kadiri, A. Ouass, Y. Essaadaoui, A. Lebkiri, *Coriandrum sativum* seeds as a green low-cost biosorbent for methylene blue dye removal from aqueous solution: spectroscopic, kinetic and thermodynamic studies, Mediterr. J. Chem., 7 (2018) 204–216.

[63] A.I. Foudah, M.H. Alqarni, A. Alam, M.A. Salkini, E.O.I. Ahmed, H.S. Yusufoglu, Evaluation of the composition and in vitro antimicrobial, antioxidant, and anti-inflammatory activities of Cilantro (*Coriandrum sativum* L. leaves) cultivated in Saudi Arabia (Al-Kharj), Saudi J. Biol. Sci., 28 (2021) 3461–3468.

[64] P. Balamurugan, G. Vinnilavu, Removal of methyl violet dye from industrial wastewater using neem leaf powder, Indian J. Ecol., 47 (2020) 442–445.

[65] K. Karthik, B. Sudhkar, P.S. Pranav, V. Sridevi, Removal of crystal violet dye from aqueous solution through biosorption using *Lysiloma latisiliquum* seed powder: kinetics and isotherm, Int. J. Eng. Res. Technol., 8 (2019) 493–497.

[66] D. Sujata, S. Shalini, G. Shashank, Evaluation of wheat bran as a biosorbent for potential mitigation of dye pollution in industrial wastewaters, Orient. J. Chem., 35 (2019) 1565–1573.

[67] A. Sharafzad, S. Tamjidi, H. Esmaeili, Calcined lotus leaf as a low-cost and highly efficient biosorbent for removal of methyl violet dye from aqueous media, Int. J. Environ. Anal. Chem., 101 (2021) 2761–2784.

[68] N.J. Okorocha, C.E. Omaliko, C.C. Osuagwu, M.O. Chijioke-Okere, C.K. Enenebeaku, Utilization of agro-waste in the elimination of dyes from aqueous solution: equilibrium, kinetic and thermodynamic studies, Int. Lett. Chem. Phys. Astron., 86 (2021) 11–23.

[69] W.C. Wanyonyi, J.M. Onyari, P.M. Shiundu, Adsorption of Congo red dye from aqueous solutions using roots of *Eichhornia crassipes*: kinetic and equilibrium studies, Energy Procedia, 50 (2014) 862–869.

[70] S. Sultana, K. Islam, M.A. Hasan, H.J. Jawad Khan, M. Azizur R. Khan, A. Deb, Md. Al Raihan, Md. Wasikur Rahman, Adsorption of crystal violet dye by coconut husk powder: isotherm, kinetics and thermodynamics perspectives, Environ. Nanotechnol. Monit. Manage., 17 (2022) 100651, doi: 10.1016/j.enmm.2022.100651.

[71] T. Nargawe, A.K. Rai, R. Ameta, S.C. Ameta, Adsorption study for removal of crystal violet dye using MMT-MWCNTs composite from aqueous solution, J. Appl. Chem., 7 (2018) 1252–1259.

[72] A. Kant, P. Gaijon, U. Nadeem, Adsorption equilibrium and kinetics of crystal violet dye from aqueous media onto waste material, Chem. Sci. Rev. Lett., 3 (2014) 1–13.

[73] M.K. Dahri, M.R.R. Kooh, L.B. Lim, Adsorption of toxic Methyl Violet 2B dye from aqueous solution using *Artocarpus heterophyllus* (Jackfruit) seed as an adsorbent, Am. Chem. Sci. J., 15 (2016) 1–12.

[74] T.C. Chandra, M.M. Mirna, Y. Sudaryanto, S. Ismadji, Adsorption of basic dye onto activated carbon prepared from durian shell: studies of adsorption equilibrium and kinetics, Chem. Eng. J., 127 (2007) 121–129.

[75] M. Alshabanat, G. Alsenani, R. Almufarij, Removal of crystal violet dye from aqueous solutions onto date palm fiber by adsorption technique, J. Chem., 2013 (2013) 210239, doi: 10.1155/2013/210239.

[76] S. Shoukat, H.N. Bhatti, M. Iqbal, S. Noreen, Mango stone biocomposite preparation and application for crystal violet adsorption: a mechanistic study, Microporous Mesoporous Mater., 239 (2017) 180–189.

[77] Y.-S. Ho, T.-H. Chiang, Y.-M. Hsueh, Removal of basic dye from aqueous solution using tree fern as a biosorbent, Process Biochem., 40 (2005) 119–124.

[78] G.K. Cheruiyot, W.C. Wanyonyi, J.J. Kiplimo, E.N. Maina, Adsorption of toxic crystal violet dye using coffee husks: equilibrium, kinetics and thermodynamics study, Sci. Afr., 5 (2019) e00116, doi: 10.1016/j.sciaf.2019.e00116.

[79] F. Mashkoor, A. Nasar, A.M. Asiri, Exploring the reusability of synthetically contaminated wastewater containing crystal violet dye using *Tectona grandis* sawdust as a very low-cost adsorbent, Sci. Rep., 8 (2018) 1–16.

[80] D.O. Omokpariola, J.N. Otuosorochi, Batch adsorption studies on rice husk with methyl violet dye, World News Nat. Sci., 33 (2020) 48–63.

[81] K. Hayat, Studies on Sorption of Methylene Blue Over *Cedrus deodara* Saw, Master of Philosophy in Chemistry, 2017, p. 97.

[82] H. Patel, R. Vashi, Adsorption of crystal violet dye onto tamarind seed powder, E-J. Chem., 7 (2010) 975–984.

[83] B. Singh, B. Walia, R. Arora, Parametric and kinetic study for the adsorption of crystal violet dye by using carbonized eucalyptus, Int. J. Comput. Eng. Res., 8 (2018) 1–11.

[84] J. López-Luna, L.E. Ramírez-Montes, S. Martinez-Vargas, A.I. Martínez, O.F. Mijangos-Ricardez, M.D.C.A. González-Chávez, R. Carrillo-González, F.A. Solís-Domínguez, M.D.C. Cuevas-Díaz, V. Vázquez-Hipólito, Linear and nonlinear kinetic and isotherm adsorption models for arsenic removal by manganese ferrite nanoparticles, SN Appl. Sci., 1 (2019) 1–19.

[85] A. Wathukarage, I. Herath, M. Iqbal, M. Vithanage, Mechanistic understanding of crystal violet dye sorption by woody biochar: implications for wastewater treatment, Environ. Geochem. Health, 41 (2019) 1647–1661.

[86] W. Handayani, A.I. Kristijanto, A.I.R. Hunga, Are natural dyes eco-friendly? A case study on water usage and wastewater characteristics of *batik* production by natural dyes application, Sustainable Water Resour. Manage., 4 (2018) 1011–1021.

[87] S. Kaur, S. Rani, R.K. Mahajan, Adsorption of dye crystal violet onto surface-modified *Eichhornia crassipes*, Desal. Water Treat., 53 (2015) 1957–1969.

[88] F. Abbasi, M.T. Yaraki, A. Farrokhnia, M. Bamdad, Keratin nanoparticles obtained from human hair for removal of crystal violet from aqueous solution: optimized by Taguchi method, Int. J. Biol. Macromol., 143 (2020) 492–500.

[89] L. Akinola, A. Umar, Adsorption of crystal violet onto adsorbents derived from agricultural wastes: kinetic and equilibrium studies, J. Appl. Sci. Environ. Manage., 19 (2015) 279–288.

[90] A. Mehmood, S. Bano, A. Fahim, R. Parveen, S. Khurshid, Efficient removal of crystal violet and Eosin B from aqueous solution using *Syzygium cumini* leaves: a comparative study of acidic and basic dyes on a single adsorbent, Korean J. Chem. Eng., 32 (2015) 882–895.

[91] D.A. Gopakumar, V. Arumukhan, R.V. Gelamo, D. Pasquini, L.C. de Morais, S. Rizal, D. Hermawan, A. Nzihou, H.A. Khalil, Carbon dioxide plasma treated PVDF electrospun membrane for the removal of crystal violet dyes and iron oxide nanoparticles from water, Nano-Struct. Nano-Objects, 18 (2019) 100268, doi: 10.1016/j.nanoso.2019.100268.

[92] J. Tariq, K. Nasir, M.L. Mirza, Kinetics, equilibrium and thermodynamics of cerium removal by adsorption on low-rank coal, Desal. Water Treat., 89 (2017) 240–249.

[93] O.J. Nnaemeka, O.J. Josphine, O. Charles, Adsorption of basic and acidic dyes onto agricultural wastes, Int. Lett. Chem. Phys. Astron., 70 (2016) 13, doi: 10.18052/www.scipress.com/ILCPA.70.12.

[94] M. Ertaş, B. Acemioğlu, M. Hakkı Alma, M. Usta, Removal of methylene blue from aqueous solution using cotton stalk, cotton waste and cotton dust, J. Hazard. Mater., 183 (2010) 421–427.

[95] S. Hong, C. Wen, J. He, F. Gan, Y.-S. Ho, Adsorption thermodynamics of methylene blue onto bentonite, J. Hazard. Mater., 167 (2009) 630–633.

[96] N. Bagotia, A.K. Sharma, S. Kumar, A review on modified sugarcane bagasse biosorbent for removal of dyes, Chemosphere, 268 (2021) 129309, doi: 10.1016/j.chemosphere.2020.129309.

[97] M. Abbaz, The removal and desorption of two toxic dyes from aqueous solution by hydroxylated hematite sand: kinetics and equilibrium, J. Appl. Chem. Environ. Prot., 2 (2017). Available at: https://revues.imist.ma/index.php/JACEP/article/view/11285

[98] P. Sun, C. Hui, R. Azim Khan, J. Du, Q. Zhang, Y.-H. Zhao, Efficient removal of crystal violet using Fe_3O_4-coated biochar: the role of the Fe_3O_4 nanoparticles and modeling study their adsorption behavior, Sci. Rep., 5 (2015) 1–12.

Supporting information

Table S1
Results the effect of pH on adsorption

pH	A_i	A_f	C_e	% age removal
1	0.307	0.266	6.0454	48.98
2	0.694	0.337	7.6591	51.34
3	0.698	0.314	7.1364	55.01
4	0.714	0.301	6.8409	57.74
5	0.701	0.256	5.8182	63.39
6	0.739	0.239	5	67.69
7	0.683	0.170	3.8636	75
8	0.753	0.219	4.9773	70.87
9	0.782	0.285	6.4773	63.51
10	0.787	0.307	6.9773	60.91
11	0.776	0.337	7.659	58.79
12	0.815	0.397	9.0227	51.67
13	0.708	0.455	10.3409	35.67
14	0.726	0.505	11.4773	30.47

Table S4
Results of experiment to study the effects of dye concentration

Dye conc. (ppm)	A_i	A_f	C_e	% age removal
5	0.622	0.207	4.0909	66.72
10	0.842	0.230	4.5454	72.74
20	1.726	0.466	9.2095	73.02
30	1.777	0.425	8.3992	76.08
40	1.845	0.523	10.336	71.65
50	1.856	0.538	10.6324	71.01
60	1.836	0.547	10.8103	70.21
70	1.843	0.551	10.8893	70.09
80	1.862	0.562	11.1067	69.84
90	1.896	0.602	11.8972	68.23
100	1.912	0.647	12.7866	66.18
120	1.922	0.670	13.2411	65.68

Table S2
Results of experiment to study the effects of adsorbent dosage

Adsorbent dose (g)	A_i	A_f	C_e	% age removal
0.1	0.852	0.273	6.0245	67.957
0.2	0.852	0.226	5.1364	73.474
0.3	0.852	0.215	4.8864	74.765
0.4	0.852	0.215	4.8864	74.765
0.5	0.852	0.215	4.8864	74.765
0.6	0.852	0.215	4.8864	74.765
0.7	0.852	0.215	4.8864	74.765
0.8	0.852	0.215	4.8864	74.765
0.9	0.852	0.215	4.8864	74.765
1	0.852	0.215	4.8864	74.765

Table S5
Results of the experiment to study the effects of temperature of the solution

Temperature (°C)	A_i	A_f	C_e	% age removal
0	1.754	0.397	7.8458	77.39
10	1.754	0.335	6.6205	80.9
20	1.754	0.399	7.8854	77.25
30	1.754	0.42	8.3004	76.08
40	1.754	0.464	9.171	73.53
50	1.754	0.781	15.4348	55.59
60	1.754	0.956	18.8933	45.59

Table S3
Results of experiment to study the effects of contact time (min)

Contact time (min)	A_i	A_f	C_e	% age removal
5	0.843	0.319	7.25	62.2
10	0.843	0.319	7.25	62.2
20	0.245	0.310	7.045	63.2
30	0.843	0.301	6.841	64.3
40	0.843	0.245	5.561	71
50	0.843	0.214	4.863	74.6
60	0.843	0.218	4.955	74.2
70	0.843	0.22	5	73.9
80	0.843	0.230	5.227	72.7
90	0.843	0.234	5.318	72.2
100	0.843	0.236	5.364	72
120	0.843	0.243	5.523	71.1

Table S6
Data of pseudo-first-order kinetic model

Time (t) min	C_e (mg/L)	q_t (mg/g)	$\log(q_e - q_t)$
5	7.25	0.09166667	–3.230993219
10	7.25	0.09166667	–3.016423414
20	7.045	0.0985	–2.838187314
30	6.841	0.105	–2.576755981
40	5.561	0.15	–2.242714356
50	4.863	0.1712	–2.139292749
60	4.955	0.16816667	–1.739292749
70	5	0.16666667	–1.563572297
80	5.227	0.1591	–1.307270553
90	5.318	0.15606667	–1.097478736
100	5.364	0.07726667	–0.929141495
120	5.523	0.14923333	–0.451656918

Table S7
Experimental data of pseudo-second-order kinetics

Time (t) min	C_e (mg/L)	q_t (mg/g)	t/q_t
5	7.25	0.09166667	54.0989
10	7.25	0.09166667	82.4992
20	7.045	0.0985	147.014
30	6.841	0.105	219.998
40	5.561	0.15	262.686
50	4.863	0.1712	293.335
60	4.955	0.16816667	361.642
70	5	0.16666667	431.779
80	5.227	0.1591	480
90	5.318	0.15606667	565.718
100	5.364	0.07726667	662.086
120	5.523	0.14923333	800.92

Table S8
Experimental data for intraparticle diffusion kinetic model

Time (t) min	$t^{1/2}$	C_e (mg/L)	q_t
5	2.236067977	7.25	0.16042333
10	3.16227766	7.25	0.15721333
20	4.472135955	7.045	0.153091
30	5.477225575	6.841	0.1482
40	6.32455532	5.561	0.1454
50	7.071067812	4.863	0.1425
60	7.745966692	4.955	0.140991
70	8.366600265	5	0.1386212
80	8.94427191	5.227	0.1366667
90	9.486832981	5.318	0.1355409
100	10	5.364	0.13424333
120	10.95445115	5.523	0.12918333

Table S9
Data of Langmuir isotherm model plot

Initial conc. (ppm) or mg/L	Initial conc. (mol/L)	C_e (mol/L)	C_e/C_{ads} (g/L)
5	1.22555E-05	1.00E-05	23.3619697
10	2.45111E-05	1.11E-05	22.2519697
20	4.90221E-05	1.37E-05	19.86309787
30	7.35332E-05	1.66E-05	16.78295304
40	9.80443E-05	1.93E-05	13.55866104
50	0.000122555	2.11E-05	11.58424134
60	0.000147066	2.25E-05	10.65962282
70	0.000171577	2.47E-05	8.58238674
80	0.000196089	2.72E-05	5.885332342
90	0.0002206	2.92E-05	4.615983193
100	0.000245111	3.13E-05	2.442811853
120	0.000294133	3.25E-05	1.358426272

Table S10
Data for Freundlich isotherm model

Initial conc. (ppm) or mg/L	$\log C_e$	$\log C_{ads}$
5	–4.998818946	–6.633512211
10	–4.953065702	–6.455360961
20	–4.876401757	–6.25590823
30	–4.845863999	–6.157654033
40	–4.796285308	–5.979894157
50	–4.744006502	–5.89698493
60	–4.717680006	–5.720024969
70	–4.673637846	–5.620457767
80	–4.615052768	–5.453946881
90	–4.565193047	–5.359457266
100	–4.51388273	–5.151540652
120	–4.488713744	–5.063719779

Table S11
Experimental data for D-R isotherm model

Initial conc. (ppm) or mg/L	$\ln C_{ads}$	ε^2
5	–16.42551888	7.888924395
10	–15.63375941	7.595175254
20	–14.95155258	7.35811538
30	–14.25748835	7.133660415
40	–13.94028451	6.969576533
50	–13.55727556	6.883990077
60	–13.33453445	6.713148702
70	–13.05080674	6.604013772
80	–12.79765977	6.579245262
90	–12.27219279	6.493460525
100	–11.86186071	6.40411314
120	–11.45964568	6.061049438

Table S12
Experimental data for thermodynamic parameters

C_e (mol/L)	$C_a = (C_i - C_e)$ (mol/L)	T (°C)	T (K)	$1/T$	$K_c = C_a/C_e$	$\ln K_c$
1.923E-05	1.223E+01	0	273	3.66E-03	636158.266	13.663
1.623E-05	1.223E+01	10	283	3.53E-03	753896.495	13.533
1.933E-05	1.223E+01	20	293	3.41E-03	632963.513	13.358
2.035E-05	1.223E+01	30	303	3.30E-03	601316.812	13.187
2.248E-05	1.223E+01	40	313	3.20E-03	544233.911	13.087
3.783E-05	1.223E+01	50	323	3.10E-03	323370.755	12.887
4.631E-05	1.223E+01	60	333	3.00E-03	264176.162	12.784

Table S13
Experimental data for desorption of crystal violet dye after using HCl

Sample	% age removal
1	70.9972
2	70.8587
3	71.2051

Table S14
Experimental data for removal of dye from tap water

Tap water	% age removal
Sample 1	72.18
Sample 2	72.44
Sample 3	71.89